Welding in the World (2021) 65:2319–2337
https://doi.org/10.1007/s40194-021-01196-y

RESEARCH PAPER

New weldable 316L stainless flux-cored wires with reduced Cr(VI) fume emissions: part 1—health aspects of particle composition and release of metals

Elin M. Westin[1] · S. McCarrick[2] · L. Laundry-Mottiar[3] · Z. Wei[3,4] · M. C. Biesinger[3,5] · I. Barker[5] · R. Wagner[6,7] · K.-A. Persson[8] · K. Trydell[8] · I. Odnevall[4,9,10] · H. L. Karlsson[2] · Y. S. Hedberg[3,4,5,11]

Received: 28 July 2021 / Accepted: 30 September 2021 / Published online: 16 October 2021

Abstract
Welding fumes have been found to be carcinogenic and stainless steel welders may be at higher risk due to increased formation of hexavalent chromium (Cr(VI)). The slag-shielded methods, identified to generate most airborne particles and Cr(VI), would potentially be most harmful. With ever-stricter limits set to protect workers, measures to minimize human exposure become crucial. Austenitic stainless steel flux-cored wires of 316L type have been developed with the aim to reduce the toxicity of the welding fume without compromised usability. Collected particles were compared with fumes formed using solid, metal-cored, and standard flux-cored wires. The size, morphology, and composition were characterized with scanning electron microscopy (SEM), energy dispersive X-ray spectroscopy (EDS), and X-ray photoelectron spectroscopy (XPS). Total metal concentrations and released amounts of metals (Cr, Cr(VI), Ni, Mn, Fe) were investigated after complete digestion in aqua regia and after incubation in phosphate buffered saline (PBS) by means of flame furnace atomic absorption spectroscopy (AAS), inductively coupled plasma mass spectroscopy (ICP-MS), and UV–vis spectroscopy. The cytotoxicity of the particles was assessed with the Alamar blue assay for cell viability using cultured human bronchial epithelial cells (HBEC-3kt). The findings correlate well with previous in vitro toxicity studies for standard and experimental wires. The new optimized 316L-type flux-cored wires showed improved weldability and generated less Cr(VI) in wt.-% than with solid wire. The respirable particles were confirmed to be less acute toxic in HBEC-3kt cells as compared to standard flux-cored wires. The highest cell viability (survival rate) was observed for the metal-cored wire.

Keywords Welding fumes · Nanoparticles · Cytotoxicity · Metal release · Flux-cored wire · Metal-cored wire · Solid wire · Austenitic stainless steel · Hexavalent chromium · Cr(VI) · Manganese

Recommended for publication by Commission II - Arc Welding and Filler Metals

✉ Elin M. Westin
elin.westin@voestalpine.com

[1] voestalpine Böhler Welding GmbH, Böhler-Welding-Str. 1, Kapfenberg 8605, Austria

[2] Institute of Environmental Medicine, Karolinska Institutet, 17177 Stockholm, Sweden

[3] Department of Chemistry, The University of Western Ontario, London, ON N6A 5B7, Canada

[4] Department of Chemistry, Division of Surface and Corrosion Science, KTH Royal Institute of Technology, 10044 Stockholm, Sweden

[5] Surface Science Western, The University of Western Ontario, London, ON N6G 0J3, Canada

[6] Linde Gases Division, Linde GmbH, Carl-von-Linde-Str. 25, 85716 Unterschleißheim, Germany

[7] UniBw Munich, Werner-Heisenberg-Weg 39, 85577 Neubiberg, Germany

[8] Swerim, Isafjordsgatan 28A, 164 07 Kista, Sweden

[9] AIMES - Center for the Advancement of Integrated Medical and Engineering Sciences at Karolinska Institutet and KTH Royal Institute of Technology, Stockholm, Sweden

[10] Department of Neuroscience, Karolinska Institutet, 171 77 Stockholm, Sweden

[11] Lawson Health Research Institute, London, ON N6C2R5, Canada

1 Introduction

Strong evidence suggests that all welding fumes can be carcinogenic and can induce chronic inflammation in the respiratory tract [1–6]. Stainless steel welders are additionally subject to inhalable hexavalent chromium, Cr(VI), reported to increase the risk of health related issues, such as lung cancer, asthma, and bronchitis [7–13]. Since the base material only contributes 5–10% to the total fume particle mass, the welding consumable composition becomes most important [14, 15]. Fillers containing more Cr typically result in aerosols with higher amounts of Cr(VI) [11, 16–19]. Other elements of concern are nickel (Ni), iron (Fe), and manganese (Mn) [20–23].

Fume can be collected and analyzed as described in, for instance, ISO 15011–1 [24], ISO 10882–1 [25], and AWS F1.2 [26]. The shape and size of the particles have a large effect on the potential absorption in the human lungs as respirable particles can be inhaled and retained [6, 27]. The most common characterization methods are scanning electron microscopy (SEM) and transmission electron microscopy (TEM) [13, 28–30]. The dominating size appears to be within 0.1–1 μm by mass, for both mild steel and stainless alloys, regardless of welding technique [10, 20, 31–34]. This aerosol range can deposit in the alveolar and bronchiolar regions of the lung [13]. Smaller particles with diameters (assuming spherical shape) ranging from 10 to 50 nm can form larger agglomerates after accumulating in the air to chainlike structures [28, 29]. Clearance of the particles in the lung depends on many parameters including site of deposition, the amount deposited, as well as size, shape, and surface reactivity [6]. Larger surface areas can influence both the reactivity and toxicity [35].

The fume composition can be determined with methods such as energy dispersive spectroscopy (EDS), X-ray photoelectron spectroscopy (XPS), X-ray diffraction (XRD), and inductively coupled plasma mass spectrometry (ICP-MS) [28, 29, 33, 36, 37]. The challenges with chemical analysis have been reviewed by Jenkins and Eagar [28] stating that elemental data from multiple techniques may not be directly compared. Extensive information is, however, gained by combining different methods for analysis [38]. While EDS analysis in SEM and TEM results in very similar bulk compositional information, XRD is mainly used to provide data on crystal structure enabling the determination of predominant oxides. XPS is ideal for analyzing the exterior layers of fume particles, where information about the composition and the chemical state can be obtained [36].

The highest emission rate and content of Cr(VI) have been confirmed for shielded metal arc welding (SMAW), but also flux-cored arc welding (FCAW) and gas metal arc welding (GMAW) generate substantial amounts of fume [34, 39]. While solid wires mainly consist of metals, trace elements, and some impurities, covered electrode coatings and flux-cored wires can contain a mixture of metals, oxides, silicates, fluorides, and carbonates. The extra components are necessary to form the slag supporting the melt and protecting the surface from oxidation. Additional binders and minerals can improve the welding characteristics, where especially potassium (K), sodium (Na), calcium (Ca), and fluorine (F) have been identified to influence the oxidation state of the particles generated [16, 28]. These elements are intentionally added for controlled fluidity, viscosity, and arc stabilization during the welding process [19]. The general solubility of the fume is significantly higher for the SMAW and FCAW processes than with GMAW [15]. This is of importance as pulmonary toxicity can be associated with soluble forms of transition metals and their doses [40, 41].

A large fraction of the fume particles has been reported to consist of oxide spinel phases, but in presence of alkali metals and fluorides, the complexity increases [28, 42]. Especially Na and K may react with Cr and oxygen (O) to form soluble chromates and di-chromates [16, 43, 44] or influence the solubility of mixed oxides containing Cr(VI) [19]. The amount of Cr(VI) has also been suggested to be higher with CaF_2, MgO, and CaO in covered electrodes [45, 46]. If eliminating the alkali and alkali-earth elements in the flux or coating, the weldability is greatly affected and the slag concept may need reformulation. Different replacements and additions aiming to reduce the fume formation and Cr(VI) content have been proposed, including rutile (TiO_2), lithium (Li), zinc (Zn), magnesium (Mg), and aluminum (Al) [16, 45–48]. The particle size of the raw materials has also been proposed to affect the arc stability and thus control both fume emissions and Cr(VI) [49, 50]. Each wire manufacturer offers unique formulations using different philosophies. Since various strips, raw materials, and coatings are applied to optimize welding conditions and feedability, also emission rates and Cr(VI) composition vary considerably [17, 18, 26].

The concentration of specific elements in the welding fume such as Cr, Mn, Na, and K can be significantly higher than what is expected from the electrode composition [16, 29]. Evaporation follows from the high temperatures reached at the electrode tip, causing vapor emission followed by condensation and oxidation [45, 51]. The temperature increases with the welding current, which results in additional fume emissions and Cr(VI) formation [18, 52]. The process parameters thus have a large effect on the formation of aerosols.

Spray arc welding with solid, flux-cored, and metal-cored wires can after parameter adjustments be performed using the same power source, but different shielding gases. The

choice of gas is important for the arc transfer, arc stability, spatter formation, material transfer, oxide formation, and loss of alloying elements, but has also been reported to affect the fume formation rate and Cr(VI) content [18, 47, 52, 53]. To improve the arc stability and retain the corrosion resistance and mechanical properties of stainless weld metals, the GMAW process is preferably welded with Ar + 2–3% CO_2 or multicomponent shielding gases containing helium. For flux-cored wires, the slag cover protects the melt and individual droplets from oxidation and the shielding gas selected for enhanced arc stability and mechanical properties is usually Ar + 18% CO_2.

To quantify to which extent a product is harmful may be complex as individual elements can be toxic or show enhanced toxicity in the presence of other elements and compounds [40, 43]. There are different ways to determine the release of metals, and for welding fumes, incubation in phosphate buffered saline (PBS) has been proven to be physiologically relevant and efficient [13, 40]. Trace metals can be analyzed using quantitative analytical methods such as atomic absorption spectroscopy (AAS), ICP-MS, and UV–vis spectroscopy [19, 54, 55].

When particles and gases enter the lungs, biological reactions may take place, possibly resulting in an inflammatory response [56]. The exposure can result in the formation of reactive oxygen species (ROS) that can produce damage to cellular membranes, proteins, and DNA [13]. Substances can also cause mutations or alterations to the genetic material and promote cancer [13, 20]. As an alternative to clinical studies and in vivo (within the living) animal testing, the effect of welding fumes can be studied in vitro (outside of an animal / "in a glass"), for instance by using cultured cells. Effects on, for instance, cell viability, DNA damage and pulmonary inflammation can be investigated by using different assays [6, 13, 19, 41, 55, 57–61].

The possibility to reach the highest productivity in all positions with the FCAW process serves as a driving force to decrease the emission rate and the amount of Cr(VI) in the welding fume. Experimental 316L flux-cored wires for reduced Cr(VI) in the fume emissions were investigated in an earlier work [55]. The results demonstrated that fumes containing lower amounts of Cr(VI) were less acute toxic regarding both cytotoxicity and DNA damage compared to the standard wires. However, inflammatory effects were observed in response to the Cr(VI) reduced fumes, likely due to the presence of other toxic components. The weldability of the wires investigated were not completely satisfactory and especially the arc stability could be improved. Therefore, the wires have undergone further development to become more user-friendly. The goal was to reduce the fume generation rate, Cr(VI) formation, and toxicity of the respirable particles as compared to the standard flux-cored wire, while maintaining the welding performance. Divided in two papers, part 1 (this paper) is focused on the health aspects of welding fume generated with the newly developed consumables as compared to solid, flux-cored, and metal-cored wires. The objective was to investigate the effect of particle morphology, composition, and release of metals on the cytotoxicity in a simulated lung environment. In part 2 [62], a round-robin test for the generation of data in fume datasheets in accordance with ISO 15011–4 [63] was conducted and discussed.

2 Experimental

2.1 Material and welding

The investigated wires included one E316LSi solid wire (SW), one standard E316LT1 flux-cored wire (FW), three new-developed E316LT1 flux-cored wires for fume reduction (FR), and one standard metal-cored wire (MC). The base metal (BM) was chosen to be the matching AISI 316L (EN 1.4404/UNS S31600). The plates had a dimension of 50 × 10 × 250 mm and all wires were of Ø 1.2 mm diameter. The chemical composition for the parent material and the filler metals is shown in Table 1.

Table 1 Chemical composition of base material and filler wires, wt.-%

	Designation*	C	Si	Mn	P	S	Cr	Ni	Mo	Cu
BM	(316L)	0.020	0.56	1.17	0.030	0.001	16.70	10.10	2.05	0.06
SW	ER316LSi	0.008	0.83	1.67	0.017	0.011	18.37	12.12	2.64	0.08
FW	E316LT1	0.022	0.72	1.53	0.024	0.008	18.68	11.86	2.72	0.12
FR1	E316LT1	0.024	0.83	1.35	0.024	0.009	18.25	11.82	2.87	0.12
FR2	E316LT1	0.023	0.79	1.31	0.023	0.009	18.20	11.60	2.55	0.12
FR3	E316LT1	0.029	0.84	1.36	0.024	0.009	18.25	11.73	2.86	0.12
MC	EC316L	0.025	0.44	1.22	0.021	0.011	18.67	12.17	2.59	0.03

*Classification in accordance with the American Welding Society standards AWS 5.9 for solid wires and AWS 5.22 for cored wires

2.2 Fume collection

Welding was carried out until a sufficient mass of particles (137–200 mg) was collected on each filter. The influence of the filter material is discussed in more detail in part 2 [62] of this paper series. In a pre-study, four different filter materials, including different cellulose and glass fiber filters, were tested on their background contamination. Triplicate samples of clean (new) filter pieces were immersed to PBS (see below) for 24 h at 37 °C (at bilinear agitation with 12° inclination and 22 cycles/min in darkness), with a background (blank) control without filter. The chosen Macherey–Nagel MN 640 w (ash content < 0.01 wt.-%) cellulose filter (Ø 240 mm) had very low levels of contamination (close to limit of detections for Fe and Ni, and below limit of detection for Cr, Cr(VI), and Mn). Fume particles were collected on these filters in a fume box as described in ISO 15011–1 [25]. The collected particles were stored for later analysis in band-heat sealed plastic bags, closed immediately after the welding.

All welding was carried out bead-on-plate with DC+ polarity and in spray arc mode. The shielding gas was Ar + 2.5% CO_2 for the solid and metal-cored wires and Ar + 18% CO_2 for the flux-cored wires. The welding machine was an EWM alpha Q 552 PULS MM RC. The wire speed was 10.0 m/min and the arc length adjusted to approximately 3 mm using high-speed imaging. The resulting welding parameters are presented in Table 2.

2.3 General sample preparation for further analysis

Filter pieces of 4 cm^2 (2 × 2 cm) size were cut from the total filter area (452 cm^2) and placed in acid-cleaned dry plastic vessels. Since the total mass of the welding fume on the entire filter area was known, the mass on the filter pieces could be calculated by (4/452) multiplied by the total fume mass on the filter, assuming equal mass distribution.

Metal release and total content measurements with triplicate samples of filter pieces with collected fume particles were exposed in parallel with a clean filter piece as background control. Background concentrations were in all cases negligible.

2.4 Fume particle characterization with SEM/EDS

Selected fume particles (FW, FR1, FR2, FR3, and MC) were characterized in terms of size, morphology, and chemical composition. Collected particles on the filter were transferred to double-sided carbon tape and coated with a 4 nm thin layer of iridium (Ir) to prevent beam charging artifacts. Examination was performed using a Hitachi SU8230 Regulus field emission microscope (FE-SEM) combined with a Bruker XFlash 6160 X-ray analyzer at an acceleration voltage of 15 kV. With secondary electron (SE) imaging, it was possible to observe variations in surface topography. The samples were also examined using EDS, a semi-quantitative technique able to detect all elements (> 0.1 wt.-%) from carbon (C) to uranium (U). Due to peak overlap for molybdenum (Mo $L_{\alpha,\beta}$) and sulfur (S K_{α}) and concentrations close to detection limits, it was not possible to unambiguously assign and quantify these elements. Sample SW was examined in a tabletop SEM (Hitachi TM1000), where the EDS only has the possibility to measure elements starting with Na and hence not O.

The ImageJ software (version 1.52v) was used to calculate the size distribution (by number) based on the SEM images (25 k magnification) for FR1, FR2, FR3, and MC by evaluating 210–290 individual particle diameters for each welding fume sample. For FW, the analysis was based on TEM images obtained in the work of McCarrick et al. [55] following the procedure described by Hedberg et al. [19].

2.5 Fume particle characterization XPS

The outermost (probing depth 7–10 nm) surface composition and oxidation states/species of the collected welding fume were determined by means of XPS. Due to their small size, this represents a significant fraction for most of the particles with information gained from both the surface oxides and the core (bulk). XPS was run for sample FW and, in a more detail, also for samples FR1, FR2, FR3, and MC. Peak assignments and quantitative chemical state analyses were done according to Biesinger et al. [64].

Table 2 Welding parameters used for collecting fume

Wire	Shielding gas	Wire feed rate, m/min	Welding speed, m/min	Arc length, mm	Stick-out, mm	I, A	U, V	Gas flow, L/min
SW	Ar + 2.5% CO_2	10.0	0.40	~3	20	265	28.2	16
FW	Ar + 18% CO_2	10.0	0.40	~3	20	190	29.1	16
FR1	Ar + 18% CO_2	10.0	0.40	~3	20	191	30.3	16
FR2	Ar + 18% CO_2	10.0	0.40	~3	20	190	29.3	16
FR3	Ar + 18% CO_2	10.0	0.40	~3	20	190	29.0	16
MC	Ar + 2.5% CO_2	10.0	0.40	~3	20	220	28.2	16

For the samples FR1, FR2, FR3, and MC, XPS analyses were carried out with a Kratos AXIS Supra X-ray photoelectron spectrometer using a monochromatic Al K(α) source (15 mA, 15 kV). XPS can detect all elements except hydrogen (H) and helium (He), and has detection limits ranging from 0.1 to 0.5 at.-% depending on the element. The instrument work function was calibrated to give a binding energy (BE) of 83.96 eV for the Au 4f7/2 line for metallic gold (Au) and the spectrometer dispersion was adjusted to give a BE of 932.62 eV for the Cu 2p3/2 line of metallic copper (Cu). The Kratos charge neutralizer system was used on all specimens. Survey scan analyses were carried out with an analysis area of 300 × 700 μm and a pass energy of 160 eV. High-resolution analyses were performed with an analysis area of 300 × 700 μm and a pass energy of 20 eV. All spectra were charge-corrected to the main line of the C 1 s spectrum (adventitious C) set to 284.8 eV and analyzed using CasaXPS software (version 2.3.14). The fume particles were fixed on adhesive C tape.

For the sample FW, an UltraDLD spectrometer (Kratos Analytical Manchester, UK) was used, with a monochromatic Al K(α) X-ray source (150 W). The fume particles were fixed on adhesive Cu tape. Wide spectra and detailed spectra (pass energy of 20 eV) for Fe 2p, Cr 2p, Ni 2p, Mn 2p, Si 2p, Bi 4f, F 1 s, O 1 s, and C 1 s (as energy reference at 284.8 eV) were run at two different locations for each sample.

2.6 Total metal content of fume particles – digestion procedure

Determination of total concentrations of Fe, Cr, Mn, and Ni was performed by digesting the cutout filter sections in 20 mL diluted aqua regia (6.9% HNO_3, 2.5% HCl, pH negative) sonicated for 2 h in an ultrasonic bath, which resulted in a final solution temperature of 60–70 °C. The digested samples were kept in the diluted aqua regia for at least 24 h prior to solution analysis. For the wires FR1, FR2, FR3, and MC, the solutions were filtered using coarse filter paper (filtering away any insoluble particles that would be a problem for further analysis) prior to ICP-MS analysis (see below). For the wires SW and FW, digested samples were directly analyzed by means of AAS (see below). In all cases, the average concentration (μg/L) of the triplicate samples, with the corresponding blank (background) concentration subtracted, was multiplied by the exposure volume and divided by the exposed particle mass (mg), to determine the μg/mg values of the total metal content (Fe, Cr, Mn, and Ni) in the fume. These values were divided by ten to obtain the wt.-% values.

2.7 Metals release from the fume particles into PBS

Filter paper pieces with collected fume from the wires FR1, FR2, FR3, and MC were immersed in 30 mL PBS (8.77 g/L NaCl, 1.28 g/L Na_2HPO_4, 1.36 g/L KH_2PO_4, adjusted with 50% NaOH to pH 7.2–7.4) in closed acid-cleaned vessels for 24 h at 37 °C with bilinear shaking (22 cycles/min, 12° inclination), followed by filtration through 20 nm Whatman Anodisc inorganic membrane filters, and acidification to a pH < 2 with ultrapure HNO_3 prior to solution analysis by ICP-MS. The procedure was identical for the wires SW and FW, except for a volume of 50 mL PBS and analysis by means of AAS after acidification.

Non-acidified samples were either frozen or directly analyzed by UV–vis spectroscopy to determine their Cr(VI) content. In all cases, the average concentration (μg/L) of the triplicate samples, with the corresponding blank (background) concentration subtracted, was multiplied by the exposure volume and divided by the exposed particle mass (mg), to determine the μg/mg values of the released metals. These values were further divided by the μg/mg total content values (previous section) and multiplied by 100 wt.-% to obtain the PBS-soluble percentage of a particular metal compared to the total content of this metal.

2.8 UV–vis spectroscopy

For the wires FR1, FR2, FR3, and MC, Cr(VI) concentrations were determined by UV–vis spectroscopy (of non-acidified samples, which were frozen if not directly analyzed). The analysis was carried out using a Cary 8454 UV–vis instrument and ChemStation software from Agilent Technologies. Polyethylene cuvettes were filled with a volume of 960-μL sample or standard solution, 20 μL 70% phosphoric acid, and 20 μL 1.0 g/L 1,5-DPC in acetone with one drop of glacial acetic acid. A blank sample (exposed in parallel, but without any welding fume) was used to correct the baseline. Quantification of Cr(VI) was conducted through a pink complex with DPC visible at 540 nm wavelength. The limit of detection was calculated to be 30 μg/L or 0.53 μg/mg of Cr(VI). The amount of released Cr(VI) in μg/mg was determined by standard calibration in a PBS matrix using 0, 58, 124, 253, 500, and 1000 μg/L, giving a linear calibration curve ($R^2 = 0.999$). The procedure was identical for the wires SW and FW, except for using a Jenway 6300 instrument. The calibration curves were based on 0, 125, 247.5, 495, and 990 μg/L Cr(VI) and linear ($R^2 \geq 0.9996$), and the limit of detection, as based on three times the highest standard deviation of the blank samples, was ≤ 10 μg/L.

2.9 ICP-MS and AAS

For the wires FR1, FR2, FR3, and MC, an Agilent 7700× ICP-MS instrument was used to measure the Fe, Ni, Cr, and Mn contents. The welding fume samples were prepared in solutions of PBS and aqua regia for a total of 32 sample solutions. The first 16 fume samples were incubated in 30 mL PBS for 24 h, as described above, after which they were filtered with 20 nm Whatman Anodisc inorganic membranes. The remaining 16 samples were digested in 20 mL diluted aqua regia (6.9% HNO_3, 2.5% HCl, pH negative) as described above. Samples in PBS were diluted four times and samples in aqua regia ten times for the analysis. The results were compared to the dilution factor adjusted method detection limit (MDL) and method reporting limit (MRL) as given in Table 3. In all cases, except the blank samples, all concentrations were significantly exceeding the MDL and MRL. The analyses were conducted by Biotron Experimental Climate Change Research Centre at Western University in London, Ontario, Canada.

The procedure was identical for the wires SW and FW, but the fume samples were analyzed by flame AAS (AAnalyst 800, Perkin Elmer, Waltham, MA). The detection limits, as estimated from three times the average standard deviations of the blank samples, were 20 µg Cr/L, 50 µg Fe/L, 40 µg Mn/L, and 10 µg Ni/L.

2.10 Cell culture and reagents

Human bronchial epithelial cells (HBEC3-kt) were cultured in 50% LHC-9 (Laboratory of Human Carcinogenesis-9, Gibco) and 50% RPMI-1640 (Roswell Park Memorial Institute, Gibco) supplemented with 1% penicillin–streptomycin (PEST, Gibco) and 1% L-glutamine in flasks precoated with 0.01% collagen (Type I, PureCol®, Advanced BioMatrix) under serum-free conditions. The cells were kept in a humidified atmosphere at 37 °C, 5% CO_2, and sub-cultured at 80% confluency. Twenty-four hours prior to exposure, cells were seeded at desired density on pre-coated plates.

Table 3 Method detection and method reporting limits in µg/L for the four different analyzed metals and four (PBS) or ten times (aqua regia) diluted samples

	^{52}Cr	^{55}Mn	^{56}Fe	^{60}Ni
MDL (Adj. 4×dilution)	0.179	0.507	2.79	0.788
MRL (Adj. 4×dilution)	0.536	1.520	8.37	2.36
MDL (Adj. 10×dilution)	0.446	1.27	6.98	1.97
MRL (Adj. 10×dilution)	1.34	3.80	20.9	5.91

2.11 Preparation of fume particles suspensions for cell exposure

Precut filters with collected fumes were weighed and immersed in 0.6 mL ultrapure water in a glass tube. The suspensions were further sonicated in a water bath for 20 min and the filter removed from the suspension and dried in a fume hood for approximately 2 h. After drying, the filter was re-weighed. The concentration of particles in the water suspension was further determined by the difference in filter weight before and after extraction. Blank filter extractions demonstrated no measurable weight loss. Fresh suspensions were prepared for each experiment and the particle suspensions were further diluted to desired concentration in cell media immediately before cell exposure.

2.12 Cell viability (Alamar blue assay)

To investigate the cytotoxic potential of the welding fume particles, the Alamar blue assay was performed. HBEC-3kt cells were seeded at 10,000 cells/well in transparent 96-well plates and exposed to welding fume particles (5–100 µg/mL) in cell medium for 24 h. The concentration of the solution was selected with 100 µg/mL as the highest possible relevant dose for inhalation and then lowered to visualize the onset of toxic effects. The Alamar blue assay was performed as previously described by Di Bucchianico et al. [65]. In brief, the exposure medium was removed and a fresh suspension of Alamar blue reagent (10 vol.-%) in cell medium was added to the wells and incubated for 2 h at 37 °C. The fluorescence was subsequently recorded by a Tecan Infinite F200 plate reader (Tecan Trading 125 AG, Mannedorf, Switzerland) at 540/590 nm excitation/emission. The average fluorescence intensity for the negative control was set to 100% viability and used to normalize the mean fluorescence values of the exposures to % viability. Three independent experiments were performed ($n=3$).

2.13 Statistical analysis

Cell viability results are expressed as mean ± standard deviation. One-way analysis of variance followed by Dunnett's multiple comparison test was used to test for significance between exposure and control ($p<0.05$). Statistical analysis and linear regression were performed using Graphpad Prism 5.02 statistical software (GraphPad Inc., La Jolla, CA).

3 Results and discussion

3.1 Release of metals

As shown in Fig. 1a, the highest total metal content was found for sample MC, but the release of metals into PBS was

closer to that of FR1, FR2, and FR3 (Fig. 1b). The largest dissolution of Cr(VI) and Mn was on contrary found for the standard flux-cored wire FW. Mn was significantly more soluble in the fume collected from the cored wires than from the solid wire SW, where instead larger amounts of Ni were released. Cr(III) was only released in small amounts into PBS from the metal-cored wire MC. Cr(III), which is not soluble at pH 7.4, has been reported to be less bioavailable and toxic than Cr(VI), which is soluble at the physiological pH [66]. Cr(VI) can as opposed to Cr(III) be absorbed in the cells where it is stepwise reduced to Cr(III) [67]. This oxidation state can interact directly with DNA or indirectly via the formation of ROS [68]. Figures 1c–f show the soluble fraction of Fe, Cr (as Cr(VI)), Ni, and Mn in PBS for the investigated welding fume samples. Fe was generally very insoluble in PBS due to the pH of the solution (pH 7.4). The Cr release as Cr(VI) was considerably smaller for the FR1, FR2, FR3, and MC samples as compared to SW and especially FW. This was also the case for Ni. For Mn, SW displays the lowest solubility, while the samples FR1, FR2, FR3, and

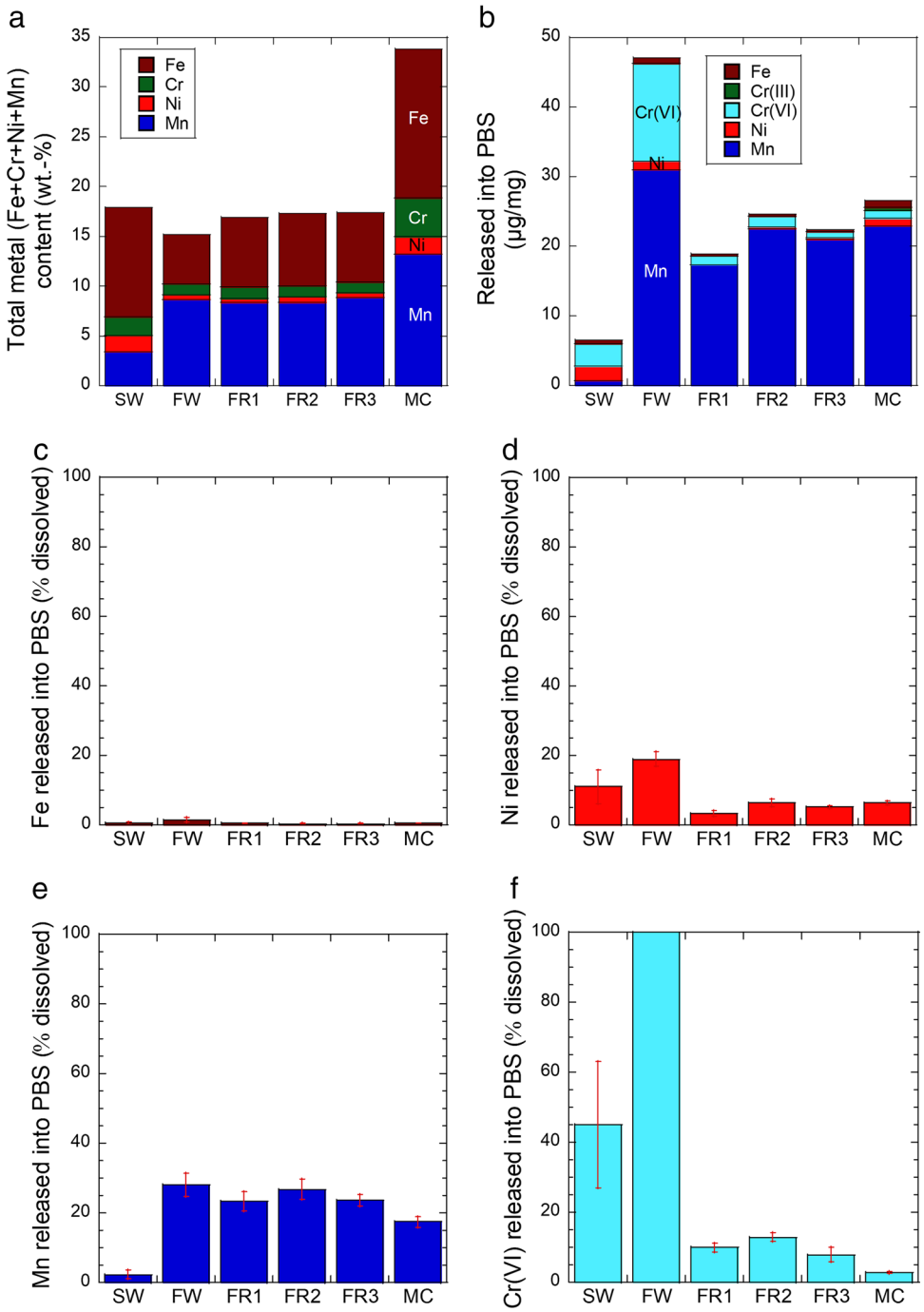

Fig. 1 **a** Total Fe, Cr, Ni, and Mn in the welding fume (determined after digestion in aqua regia). **b** Released amount (µg/mg) Fe, Cr(III), Cr(VI), Ni, and Mn into PBS (37 °C, 24 h). Released **c** Fe, **d** Ni, **e** Mn, and **f** Cr(VI) into PBS (37 °C, 24 h) as percentage of total Cr, Mn, Fe, and Ni in the welding fume (100% means complete dissolution of that element)

MC have comparable or slightly lower solubility than the standard flux-cored wire sample FW. An almost complete dissolution (100%) of Cr as Cr(VI) into PBS was observed for the sample FW. Whether any Cr was still insoluble in that case cannot be stated with confidence due to associated uncertainties (about 20%) of the trace metal analysis and a possible incomplete digestion in aqua regia (for total Cr estimation). However, it is clear that the solubility of Cr for FW is high and far higher compared to the other samples.

3.2 Detailed particle characterization

SEM investigations of the fume particles confirmed the dominance of nanometer-sized particles (Fig. 2). Compositional EDS findings are summarized in Tables 4 and 5 and in Fig. 3. Sample SW showed particles rich in the main alloying elements (Fe, Cr, Ni, Mn, Mo). All cored wires generated Cr, F, Fe, Mn, and Si, but only the flux-cored wires showed bismuth (Bi) in the fume. Higher amounts of K and Na were observed in sample FW, the sample with the highest Cr(VI) solubility, but Ni was found to be below the detection limit. Sample MC contained less F, Ti, Mo, and Bi, and more Mg, as compared to samples FR1, FR2, and FR3.

Few single micrometer-sized particles were also present in the welding fume. Their composition varied considerably, suggesting different origins (both flux particles and main alloying elements) (Fig. 4). The flux-cored wires contributed both slag formers (TiO_x and $(Ti,Zr)O_x$) and metal oxides with primarily Fe, Mn, Ni, and Cr. The metal-cored wire showed metal oxides with Fe, Cr, Mo, Ni, and Mn, as well as Mg/Ca-rich particles. Most of the metal oxides are suggested to exist as Fe oxides with some substitution of other metals in their matrix. The Ti-rich particles are most likely rutile TiO_2 used in the flux for slag formation.

Figure 5 shows the SEM image determined particle diameter size distribution of the welding fume in samples FR1, FR2, FR3, and MC. For comparison, the TEM-derived size distribution for sample FW is also included, although these particles are naturally smaller due to a selection bias in the sample preparation. Sample MC was slightly smaller in size,

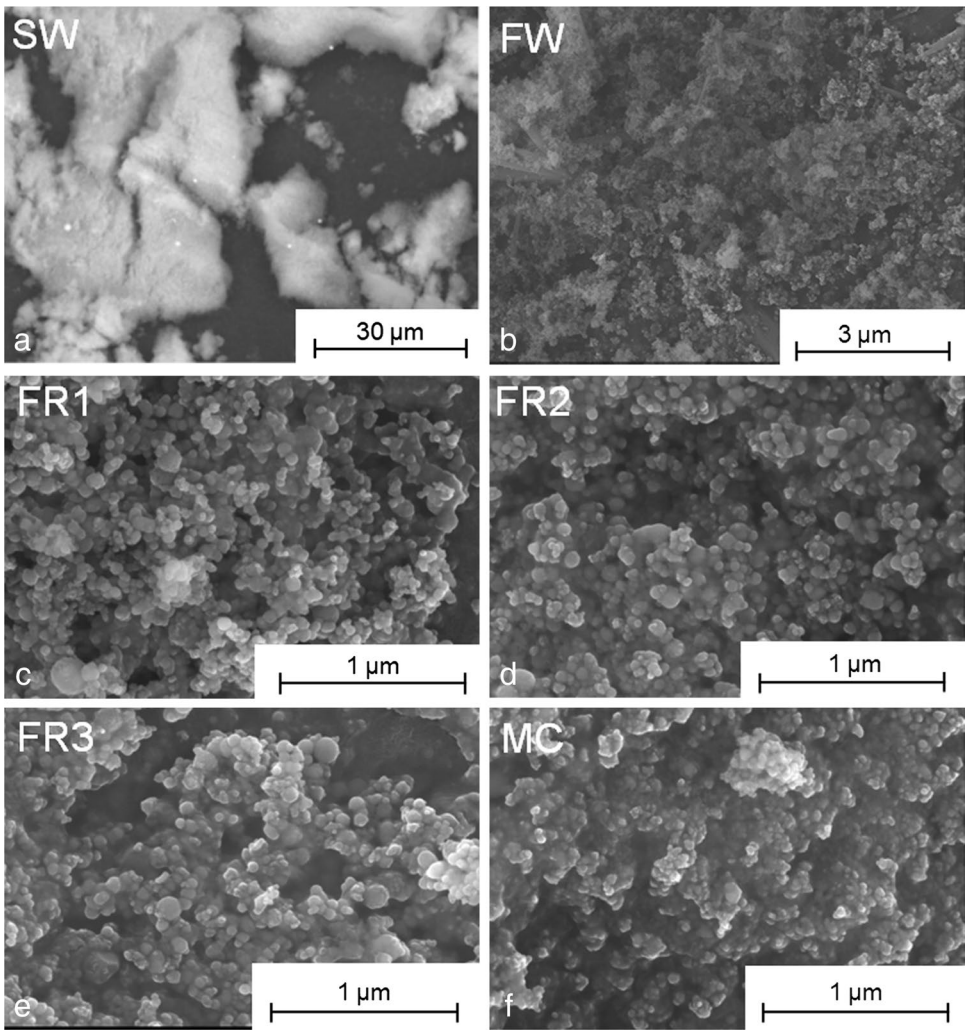

Fig. 2 Overview SEM images at magnifications 2.5 k (SW), 10.0 k (FW), and 50.0 k (FR1, FR2, FR3, and MC). The images were acquired with two different SEM instruments having various resolution capabilities

Table 4 EDS compositional analysis of welding fume particle aggregates, in wt.-% with carbon excluded (the particles were mounted on carbon tape). Mean values and standard deviation of 3–5 different areas are shown. Note that only the composition of the aggregates, not the micrometer-sized particles, is included

Wire	O	F	Na	Mg	Al	Si	S	K	Ca	Ti	Cr	Mn	Fe	Ni	Zr	Mo	Bi
FW	42±13	7.8±2.2	13±5.0	-	0.94±0.29	8.2±2.4	0.39±0.77	4.5±1.6	-	0.83±1.2	4.7±2.0	9.2±3.9	6.1±2.8	-	-	0.62±1.2	0.90±1.8
FR1	27±5.9	12±6.7	4.3±2.1	-	2.1±1.5	9.8±6.1	-	0.44±0.15	-	1.2±0.66	7.6±4.2	13±7.4	15±8.4	2.4±1.1	-	1.3±1.2	3.1±2.1
FR2	41±3.3	13±3.7	4.8±1.1	-	2.0±0.40	6.7±1.5	-	0.34	0.1	1.4±0.26	5.6±0.60	9.7±1.9	11±0.79	2.1±0.17	-	1.1±0.43	1.8±0.55
FR3	32±6.4	17±2.4	4.3±0.98	-	2.1±0.50	7.8±3.1	-	0.32±0.080	-	1.6±0.52	6.1±2.1	12±4.3	11±3.3	2.1±0.68	-	0.64±0.42	2.6±1.2
MC	40±3.0	7.2±0.95	3.1±0.44	4.8±1.6	1.0±0.44	3.6±1.2	0.50±0.23	0.50±0.17	0.39±0.095	-	7.2±2.1	12±3.5	17±4.4	2.5±0.44	1.2±0.23	-	-

with a peak around 50–60 nm, as compared with samples FR1, FR2, and FR3, being predominantly about 80 nm. The size distribution of welding fume particles depends on the method used for detection, as it spans all the way from very small (< 20 nm) to micrometer-sized, with the majority of particles (by number) being smaller than 100 nm.

3.3 Surface composition measured by XPS

The surface compositions (based on XPS survey data) for the FR1, FR2, FR3, and MC fume particles are summarized in Table 6. The results are consistent with the EDS findings with less F, Bi, and Ti, and more Mg for sample MC compared with samples FR1, FR2, and FR3.

The XPS high-resolution data for samples FR1, FR2, FR3, and MC are summarized in Tables 7, 8, 9 and 10. Mn was primarily detected in its divalent and trivalent form, with little or no contribution from the tetravalent form. Cr was entirely present in its trivalent state, as an oxide and/or hydroxide. A large fraction of the O signal can be attributed to SiOx or organic O compounds. F was only present as fluoride species and Bi in its trivalent form (probably from added Bi_2O_3) [68].

No Ni was observed for sample FW. Fe and Ti were possibly present, but interfered with the F 1 s loss structure and Bi 4d peaks, respectively. Even though the signal to noise ratio was low for Cr, Mn, Ti, and Fe, it was evident that Mn was present in its divalent (74 at.-%), trivalent (19 at.-%), and tetravalent (6 at.-%) forms. Bi was found as Bi(III). The Si peak position indicated the presence of both silica and organic silicon. Fluoride was detected. The O peak could originate from oxide, hydroxide, or defective oxide, as well as oxygen in silica compounds and organic compounds (e.g., adventitious oxidized C).

In all, the compositional XPS analysis of sample FW was very similar to observations for the samples FR1, FR2, and FR3, except that the oxidation state of Cr could not be identified due to low signal to noise ratio. It can be assumed that its oxidation state is at least partially Cr(VI), as previously observed for similar samples [19]. No evidence of Cr(VI) in the outermost (7–10 nm) surface was obtained for either FR1, FR2, or FR3.

3.4 Toxicity

The effects on cell viability following welding particle exposure for 24 h, assessed by the Alamar Blue assay, are shown in Fig. 6. Exposure to all samples tested, except sample MC, resulted in a dose-dependent decrease in viability. The largest effect was observed in response to sample FW, resulting in a statistically significant decrease in viability starting at 25 µg/mL ($p < 0.001$). Samples SW, FR1, FR2, and FR3 resulted in comparable cytotoxic effects of 50–60% viability

Table 5 EDS results for the SW fume. Mean values and standard deviation of three different areas are shown. Note that only the composition of the aggregates, not the micrometer-sized particles, is included. O was not detectable with this instrument

Wire	F	Al	Si	S	Cr	Mn	Fe	Ni	Cu	Mo
SW	0.33 ± 0.29	0.40	4.3 ± 0.10	0.23 ± 0.15	18 ± 0.26	12 ± 1	53 ± 0.68	9.5 ± 0.44	0.67 ± 0.65	2.0 ± 0.46

at the highest dose tested ($p < 0.01$). No cytotoxicity was observed in response to sample MC.

When comparing the survival rate of human bronchial epithelial cells exposed to welding particles to the soluble Cr(VI) (in PBS) of the same particles (Fig. 1b), it becomes apparent that there is an association between these two parameters. In McCarrick et al. (2019), Cr(VI) release in PBS was shown to predict the cytotoxic effect of the welding fumes in human bronchial epithelial cells to a large extent. To follow up these results, a compilation of results from the present study and previously published [19, 55, 61] was made, which confirmed the same linear correlation where (cyto)toxicity is increased with increased amount of soluble Cr(VI) in PBS, and vice versa (Fig. 7). No correlation was found with the other metals (Fe, Mn, Ni), with $R^2 < 0.30$.

3.5 Weldability

Depending on the type of application, local preferences, and requirements, different flux-cored wire electrodes may be preferred. In this work, it was decided to develop a product with fast-freezing slag for welding in all positions. This type of wire is most universal and has been reported to generate the lowest levels of fumes in FCAW [18, 69].

When introducing Cr(VI)-reduced products on the market, it is of course important that these show an acceptable weldability. Although the first set of experimental Cr(VI)-reduced wires used for the work of McCarrick et al. [55] showed significantly lower toxicity than the standard flux-cored wires, the weldability may not have been sufficiently satisfactory to convince all users. Welders aware of health risks with standard products may accept some deterioration in the conversion, but could be more motivated to use additional personal protection equipment such as helmets with breathing apparatus than a wire causing more rework and grinding. When evaluating the suitability for a new product, there are a few critical aspects to take into consideration. The arc transfer and stability affect the spatter formation, and the slag cover is crucial for support. Excessive fluid melts may be challenging to weld out of position, while too viscous melts can cause uneven bead shapes and slag entrapment. The slag should cover the whole weld bead, be easy to remove, and not leave any residuals after hand brushing the surface. Since most slag ends up on the floor, a too thick slag cover affects the recovery rate and thus the total productivity. If the slag becomes too thin, it can come off in small flakes at high velocity and burn the welder's skin and eyes. All operators will appreciate if the process parameters are easy to find and if the wire allows for high welding speed without causing any disturbances. The goal with the new wires was to optimize the fume formation rate and reduce the Cr(VI) content without compromising the weldability. The outcome was significantly improved weldability as compared to the previous generation of Cr(VI)-reduced wires, despite elimination or substitution of key components known to be beneficial for arc stability and slag removal.

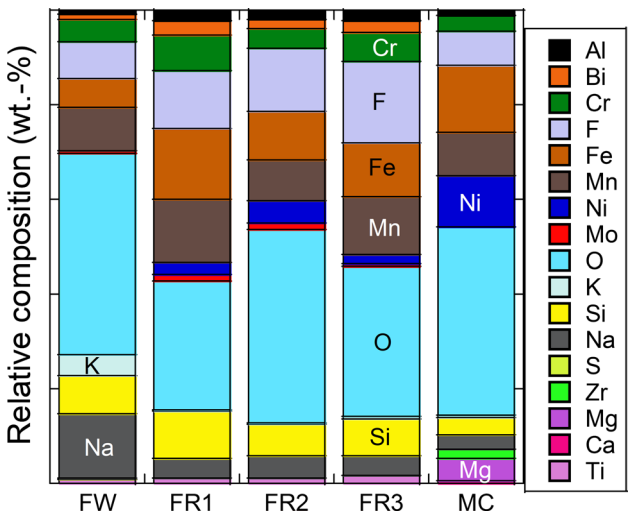

Fig. 3 Relative elemental composition (excluding C) in weight percent of the welding fume determined by SEM/EDS

3.6 Welding fume particles – morphology and composition

All welding fume from the cored wires showed larger agglomerates of tree-like coral shape as previously described by Kirichenko et al. [70]. The particle size (by number) distribution ranged as expected from a few nanometers up to a few micrometers. Visually, the samples were very similar, but sample MC showed somewhat smaller size than the samples FR1, FR2, and FR3. Jenkins et al. [30] and Keane et al. [34] made similar observations for the mass median aerodynamic diameter of fume generated by the GMAW process as compared to FCAW. Hedberg et al. [19] found larger nanoparticles for flux-cored wires than solid wires of the same alloy type.

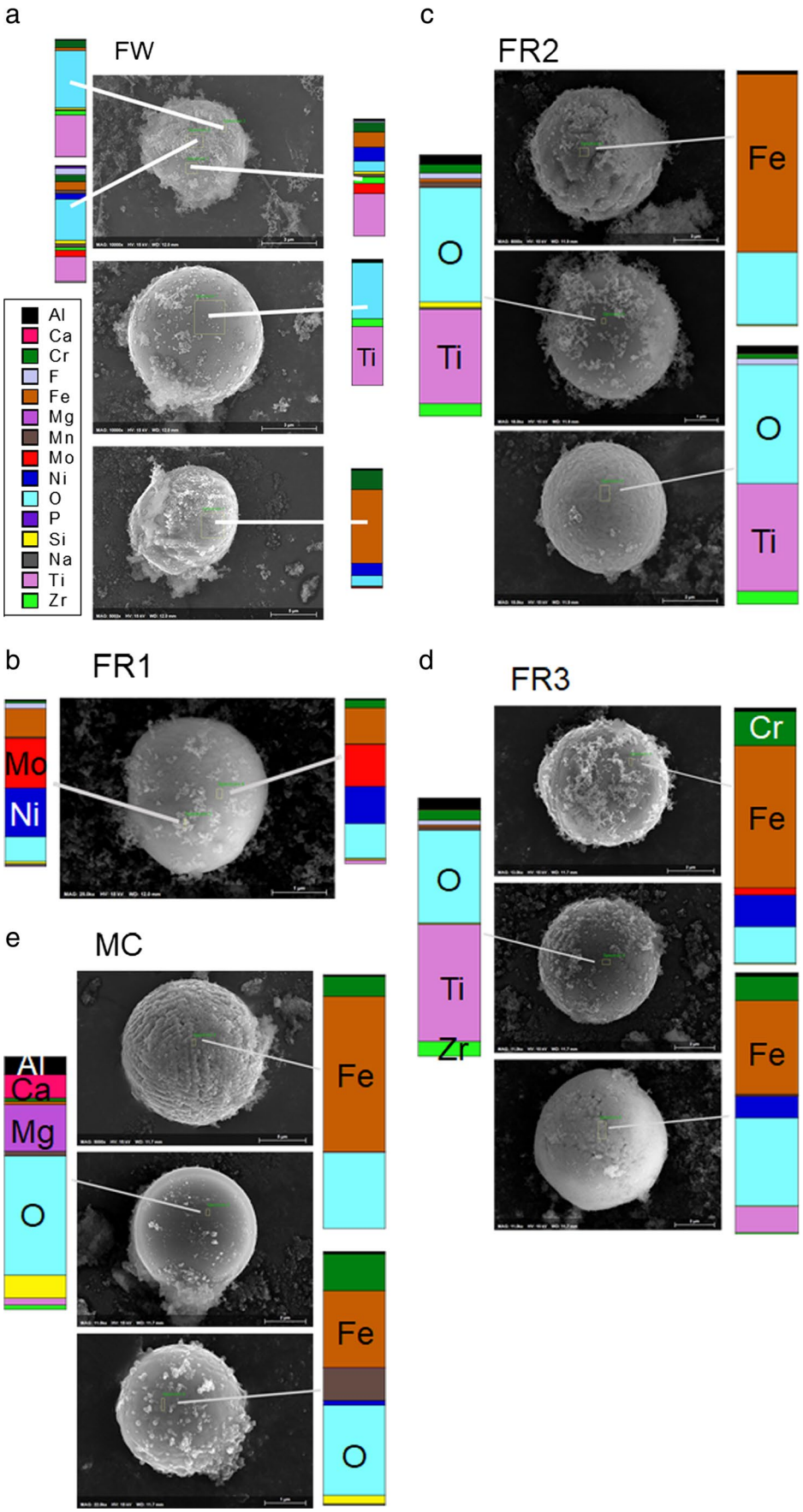

Fig. 4 SEM images of micrometer-sized particles in welding fume with relative elemental compositions (excluding C) in weight percent measured by means of EDS

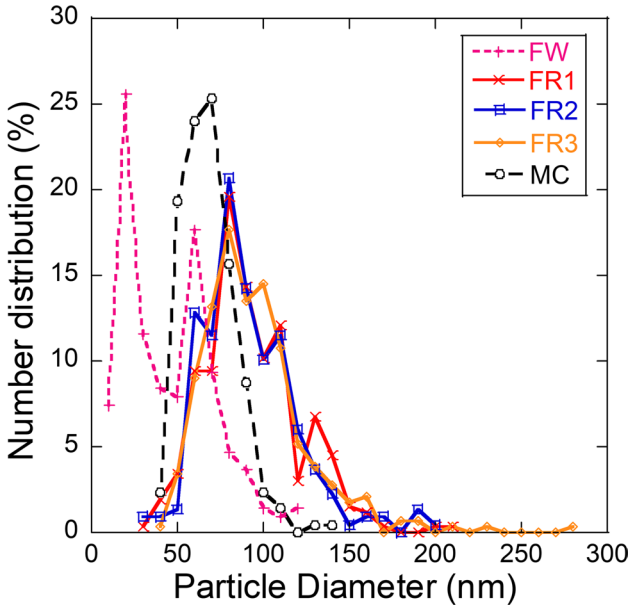

Fig. 5 Size distribution (by number) of welding fume particle diameters determined from × 25 k magnification SEM images (primary particles in aggregates only, no micrometer-sized particles included) for samples FR1, FR2, FR3, and MC. The size distribution of the sample FW is derived from TEM images and hence naturally smaller due to a selection bias, necessary in TEM sample preparation. No data is available for sample SW

Berlinger et al. [31] saw a correlation between chemical composition and particle size, with increasing amounts of volatile elements with larger diameters and related this to different formation mechanisms. Sowards et al. [38] studied the fume generated by covered electrodes of E308-16 type and found that the fractions of Na decreased and Si increased with the particle size. The surface composition is often quite different from the bulk and contains considerably larger fractions of volatile elements such as Na, K, F, and S [31, 43]. Particles have been reported to mainly consist of metal oxides such as $(Fe,Mn)_3O_4$ for mild steel and $K_2(Cr,Mn,Fe)O_4$, when using stainless steel-covered electrodes, while the shell (surface) consists of more elements and compounds such as SiO/SiO_2, NaF and CaF_2 originating from flux-based processes [43]. When present, chromates appear to be condensed on the surface of the metal oxide particles [20]. This may influence the toxicity as the outer layers are most likely first to interact in the body after ingestion or inhalation [36]. Especially Na and K readily react with Cr and O forming soluble chromates such as Na_2CrO_4 and K_2CrO_4 [16], but also, other Na and K-rich chromates and di-chromates have been observed [43, 44]. The FW fumes contained significant amounts of Na and K, while lower concentrations were detected for the newly developed flux-cored wires (FR1, FR2, and FR3) and minor levels with MC. Although solid wires are not alloyed with alkaline constituents, Cr(VI)

Table 6 Results of XPS bulk analyses in at.-%

Wire	Al	Bi	C	Cr	F	Fe	K	Mg	Mn	Mo	N	Na	O	Si	Ti	Ni
FR1	0.3	0.3	24.7	1.0	24.6	0.4	-	-	2.0	0.1	0.6	8.4	31.1	6.1	0.1	-
FR2	0.3	0.3	32.2	0.8	18.1	0.5	-	-	1.7	0.1	0.6	6.4	33.4	5.3	0.1	-
FR3	0.2	0.3	35.8	0.7	19.3	0.2	-	-	1.5	0.1	0.7	6.0	30.6	4.3	0.1	-
MC	0.1	-	37.2	1.2	9.1	2.5	0.2	1.9	3.0	< 0.1	0.9	2.5	38.4	2.7	-	< 0.1

Table 7 Proportion of Mn, Cr and O species as identified by XPS, at.-%

Sample	Mn			Cr		O		
	Mn_2O_3	MnO	MnO_2	$Cr(OH)_3$	Cr_2O_3	Hydroxide	Oxide	SiO_X, organic O
FR1	1.0	1.0	0	0.2	0.8	6.3	2.3	23
FR2	0.6	1.1	< 0.1	< 0.1	0.7	5.9	5.7	22
FR3	0.7	0.8	0	0.2	0.6	4.2	3.3	23

Table 8 Proportion of C, Si, F, and Bi species as identified by XPS, at.-%

Sample	C				Si			F	Bi
	C–C, C-H	C–OH, C–O–C	C = O	O-C = O	SiF_x?	Silica, silicate?	Silicone/ siloxane	Fluoride	Bi(III)
FR1	9.6	12	2.8	0.8	0.9	0.8	4.4	25	0.3
FR2	15	13	3.5	1.0	0.4	0.6	4.3	18	0.3
FR3	15	16	4.3	0.9	0.7	0.7	3.0	19	0.3

Table 9 Proportion of of Fe, Mn, and Cr species as identified by XPS, at.-%

	Fe				Mn			Cr	
Sample	Fe_2O_3	$Fe_3O_4^{II}$	$Fe_3O_4^{III}$	FeOOH	Mn_2O_3	MnO	MnO_2	$Cr(OH)_3$	Cr_2O_3
MC	1.0	0.4	0.8	0.3	0.2	2.8	0	0.1	1.1

was still observed in the fumes. It has been suggested that these may instead originate from the Ni or Mn chromates, $NiCrO_4$ and $MnCrO_4$ [43]. Cr(VI) has also been shown to be included in mixed, possibly amorphous, oxides [19].

3.7 Metals release and effect on toxicity

The viability of lung epithelial cells after exposure to various concentrations of welding particles indicate that the new flux-cored wires may be significantly less toxic than the standard flux-cored wire, on the level or somewhat better than solid wire. This is in agreement with the previous work presented by McCarrick et al. [55]. The differences between FR1, FR2, and FR3 were small, which means that any of these wires can be a possible substitute to FW when needed. As compared to the use of GMAW, substantially higher welding speeds may thus be reached without increasing the risk for exposure. As an important new finding, the MC wire did not indicate any cell death under the investigated doses and conditions. Reasons behind could be more favorable temperatures and arc stability influencing the composition (e.g., the manganese speciation) in the formed fume particles. With these encouraging results, the MCAW process may be considered as an alternative to both GMAW and FCAW where applicable.

McCarrick et al. [55] concluded earlier that the new Cr(VI)-reduced flux-cored wires were considerably less cytotoxic and did not cause any significant DNA damage at the doses tested. However, the new wires were found to cause rather similar inflammatory effects compared to standard FCW as assessed by cytokine release of human monocyte-derived macrophages [55]. This suggests that the presence of other harmful metal components than Cr(VI), such as Mn, also contribute to the toxicity of welding fume particles. As previously shown, no correlation was observed between cytotoxicity and release of Mn, but Mn release was well correlated to the acellular ROS production [61]. This is in agreement with Antonini et al. [40], concluding that the effect of soluble Cr from stainless covered electrodes on ROS production was low and that other metals may have a larger effect. Yu et al. [71] concluded that many welding fume components generated from SMAW of stainless steel were associated with ROS production, including Cr(VI), Mn, Fe, and various gases (O_3, NO_2, and nitrous fumes). Leonard et al. [13] studied the effect of particle composition and morphology on the generation of free radicals, ROS, and ROS-related damage. Fume formed in GMAW of stainless steel caused more DNA damage than mild steel due to the presence of Cr and Ni. The greatest free radical generation was observed when analyzing ultrafine particles, which agglomerated in large chains, generating a larger surface area where reaction can take place. McNeilly et al. [41] found Ni-based SMAW to induce significant production of ROS in A549 cells.

The toxicity of the fume is not determined solely by the metal composition but also on the release of the metals [61]. Previous studies have suggested the soluble fraction of stainless steel fume particles to play an essential role in the toxicity [40, 41, 55, 60, 72]. Other elements than Cr(VI) can cause acute systemic inflammatory responses and there may be co-exposure with other carcinogens such as Ni and NiO [14, 73]. Badding et al. [57] compared the cytotoxicity and oxidative stress of fumes generated with a Ni-Cu-based consumable, intended to replace mild steel and stainless fillers. Although significantly lower Cr(VI) and Mn contents were confirmed, the cell viability was reduced and more DNA damage observed. This could partly be due to formation of more Ni in the fumes and the authors concluded that the replacement material instead could be more toxic. Ni compounds have been demonstrated to cause oxidative DNA damage and be carcinogenic [22]. Also, Cu-containing nanoparticles are highly toxic to lung cells [74].

In studies carried out in vivo, Fe oxide (Fe_2O_3 but not Cr_2O_3, $CaCrO_4$, or NiO) was reported to cause long-term effects such as siderosis (pigmentation in the lungs) and to promote lung tumors [9, 32, 75, 76]. In addition, particles may be transported from the lung via the lymphatic and circulatory system to other parts of the body where the toxic effects may be manifested [20].

Mn in welding fumes can be present in different oxidation states, but is primarily reported as (II) and (III) in the oxide spinel phase [28, 42]. Both have been proposed to increase the dose-dependent formation of ROS, with the trivalent form being most potent [77]. The welding parameters in GMAW of stainless steel have been suggested to affect the valence states and thus affect the toxicity of Mn [78, 79]. Keane et al. [78] found MnO, MnO_2, and Mn_3O_4 in welding fumes formed when welding stainless steel with the GMAW process, but the amounts varied with the process parameters. The dominating Mn fraction was in oxidation state (II), but depending on the arc mode and shielding gas, also phases with oxidation states (III) and (IV) were observed. In the current study, the predominating fraction was shown to be Mn(II), followed by Mn(III).

Table 10 Proportion of O, C, Si, and F species as identified by XPS, at.-%

	O			C				Si		F
Sample	Hydro-xide	Oxide	SiOx, organic O	C–C, C-H	C–OH, C–O–C	C=O	O-C=O	SiF_X?	Silica, silicate?	Silicone/siloxane	Fluoride
MC	5.2	9.6	24	16	16	4.3	1.3	0.1	0.4	2.1	9.1

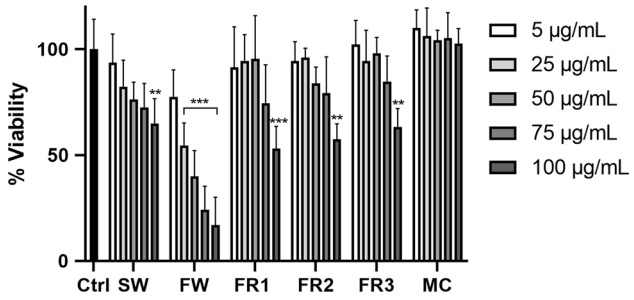

Fig. 6 Cell viability of HBEC-3kt cells following 24 h exposure to welding fume particles assessed by the Alamar Blue assay. The results are presented as mean ± SD of three independent experiments. Asterisks indicate a significant (*$p < 0.05$) reduction in cell viability compared to control (100% viability). Ten percent DMSO was used as a positive control and significantly reduced cell viability (*$p < 0.05$, **$p < 0.01$, ***$p < 0.001$)

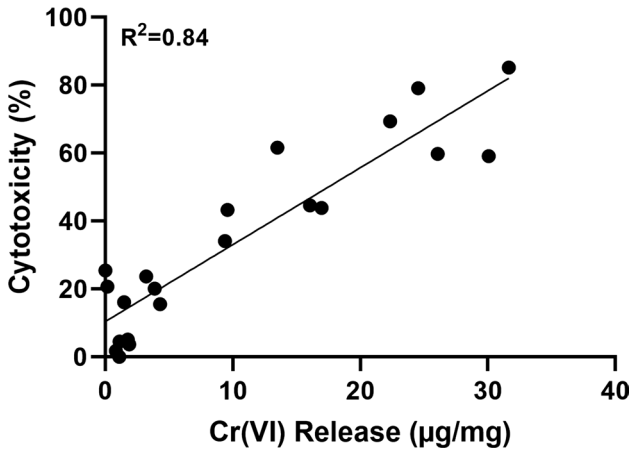

Fig. 7 Regression between release of Cr(VI) from welding fumes and toxicity. Linear regression between the Cr(VI) release in PBS per fume mass and cytotoxicity observed after exposure to 50 µg/mL of welding particles for 24 h. Results from the present work combined with earlier work [19, 55, 61]

Only sample FW contained small amounts of Mn(IV). This may be highly relevant as the various manganese oxides have different solubility and toxicity. In the presence of fluorides and potassium, $KMnF_2$ and K_2MnO_4 may form [80]. Antonini et al. [40] pointed out that fluorides present in covered electrodes may affect the toxicity of welding aerosols. It was also stated that freshly generated stainless steel welding fume more readily induces lung inflammation in rats as compared to aged fume. The fume emission samples in this work were not investigated immediately upon collection, which may have affected the quantitative results somewhat, though the ranking is believed to be unaffected by storage.

3.8 Protection of welders

Although stainless steel generates considerably more Cr(VI) than unalloyed and low-alloyed steel, mild steel welders have also a higher risk of developing severe health issues such as lung cancer, pulmonary fibrosis, acute respiratory infections, and cardiovascular diseases [3, 12, 32, 43, 56, 81, 82]. Additional exhaust may form during other tasks a welder may perform, such as thermal cutting, grinding, and arc gouging [14, 83]. Fume can also be generated when welding painted, coated, or galvanized materials [84]. It is thus always important to ensure good ventilation, provide respiratory protection such as fresh-air supplying masks where needed, and to train the welders on risks and different protective measures.

It should be noted that there is a large difference between self-shielded and gas-shielded flux-cored wires, as the former needs to generate its own shielding gas [46, 52]. More microspatter forms with the self-shielded type due to arc instabilities, similar to gas-shielded wires welded with 100% CO_2 as shielding gas.

The work environment affects the total exposure to airborne particles. As an example, a boiler maker is exposed to significantly higher amounts of fume and Mn than a pipefitter. Confined and restricted spaces increase the need for local exhaust ventilation and personal respiratory protection as compared to working in open space or outdoors [33, 79]. Various recommendations and binding occupational exposure limits exist in most industrial countries to protect workers, and are becoming increasingly stricter as more research is made available [14, 85–88]. This serves as motivation for companies to select welding processes and consumables generating lower levels of harmful elements, but also to increase the extent of mechanization and invest in suitable ventilation. It may also push for more health-driven innovation on personal protection equipment and fume extraction systems. Fresh air supplying welding helmets and special integrated extraction torches are already available on the market [53].

When the regional specifications restrict potential exposure to general fume, Cr(VI) and/or Mn even further, the manufacturers have to consider other alternatives. As the quantity and constituents of fumes vary with the welding methods, conversion to other processes may contribute to reduced exposure [89]. Among available processes, submerged-arc welding (SAW) results in the lowest formation of fume, ozone (O_3), and UV-radiation. At the same time, the highest deposition rates and productivity can be achieved. Some disadvantages to consider are that the method is limited to welding of plates in flat and horizontal positions and that another process may be needed for the root pass. Gas tungsten arc welding (GTAW) can be used in all welding positions, yielding the highest mechanical properties, but the process is slow and thus more time-consuming. It is the cleanest manual method when it comes to welding fume, but substantial amounts of O_3 are generated, which is highly inflammatory and can cause different pulmonary edema and DNA damage [15, 20, 90]. Wagner et al. [91, 92] have, however, shown that it may be possible to reduce the O_3 formation considerably with the GTAW process by selecting special shielding gases.

Decisions on the welding procedure specification can have a great effect on the formation of airborne particles. Since some of the processes represent lower deposition rates, the total amount of fume generated to complete a weld should also be considered [53]. If there is an option to mechanize the process, this would keep the operator further away from the exposure source. The choice of shielding gas affects the generation of welding fume. While the majority of the flux-cored wires have dual classifications and can be run on both mixed gas and on straight CO_2, Ar + 18–25% CO_2 typically results in the most attractive surface appearance, highest toughness, and lowest FER [18, 26, 83, 93]. The fume generation rate is also increased with the current [18, 52], which the welding engineer can limit if the loss of productivity is acceptable [94].

The potential to change to a wire generating less Cr(VI) may be another alternative. For most alloys, a matching solid wire is available. Although the same welding machine can be used, the GMAW process may require pulsing and special shielding gases to reach a good result for certain alloys. For some stainless steels, solid wires are more prone to spatter formation and porosity than cored wires, why more advanced power sources may be required. As seen in this study, the metal-cored wire released far less Cr(VI) in PBS than the solid wire, but also have many of the advantages of the flux-cored wires. The cored wires enter the favorable spray arc droplet transfer mode at a much lower wire feed rate than solid wires [95]. In many applications, significantly higher welding speed and productivity can be achieved. Similar to the solid wires, the spray arc needs to be pulsed when welding out of position with metal-cored wires and the process becomes fairly slow as compared to FCAW. An evident risk of changing to a welding method, which results in lower productivity, is that the engineering companies decide to relocate the production to other countries (with less strict occupational hygiene limits) to remain competitive.

4 Conclusions

Austenitic flux-cored wires of E316LT1 type have been developed to reduce the amount of Cr(VI) in the fume emissions. Aerosols generated from the new consumables were compared to those formed when welding solid, standard flux-cored, and metal-cored wires. The collected particles were subject to investigation with SEM and XPS, where the

morphology and more detailed compositions were analyzed. The release of metals was studied after incubation in PBS at 37 °C, an environment simulating the conditions of body fluids and suitable for Cr(VI) analysis. The cytotoxicity of the particles with focus on the viability of lung cells was assessed with the Alamar blue assay using cultured human bronchial epithelial cells (HBEC-3kt).

Characterization suggests most particles to be in the nano-range and hence respirable, but the composition varied between the different products. Flux-cored wires contributed Na, K, F, Ti, Zr, and Bi, which were not found or only available in small amounts for the solid wires, while the metal-cored wire was unique in that it resulted in some Ca and Mg. Few micrometer-sized particles were also present in the collected aerosols from all wires. These were primarily metal oxides and metals covered with metal oxides, but for the flux-cored wires, additional slag particles were found.

The new wires generated considerable less Cr(VI) than the standard flux-cored wire and the weldability has been improved in terms of arc stability, control of melt, and slag removal as compared to previously investigated Cr(VI)-reduced wires.

The solubility of Cr, Cr(VI), Mn, Ni, and Fe affected the toxicity and a linear correlation between cytotoxicity and Cr(VI) release was found. The standard flux-cored wire showed the largest release of Cr(VI) and Mn into PBS and a corresponding decrease in cell viability could be confirmed. Significant amounts of Cr(VI) and Ni were released for the solid wire, while the fume-reduced flux-cored wires instead contained substantial amounts of Mn. Despite the obvious difference in metal composition and release, the toxicity of these wires was relatively similar. The fume generated by the metal-cored wire also contained and released large amounts of Mn and some Ni, but had no negative effect on the survival rate of the cultured human bronchial epithelial cells.

In all, weldable alternatives to a standard 316L flux-cored wire have been developed, which result in fumes with significantly lower cytotoxicity, emission, and soluble Cr(VI). As Mn and other potentially hazardous metals are still present, inflammatory and long-term health effects should not be disregarded. Good ventilation and personal protection are always important during welding operations.

Acknowledgements Juliette Theodore (KTH Royal Institute of Technology) is greatly acknowledged for experimental help. The contribution from Andrea Maderthoner at voestalpine Böhler Welding and the team of Global R&D Joining Cored Wires for wire development and testing is highly appreciated.

Author contribution Conceptualization: Hedberg YS, Karlsson HL, McCarrick S; methodology: McCarrick S, Barker I, Biesinger MC, Wei Z, Hedberg YS, Karlsson HL, Westin EM; formal analysis and investigation: McCarrick S, Barker I, Laundry-Mottiar L, Biesinger MC, Wei Z, I. Odnevall I, Hedberg YS, Westin EM, Wagner R; writing – original draft preparation: Westin EM, Hedberg YS; writing – review and editing: all authors; funding acquisition: Hedberg YS, Karlsson HL, Persson K-A, Odnevall I; resources: Westin EM, Wagner R; supervision: Hedberg YS, Karlsson HL. All authors have read and agreed to the published version of the manuscript.

Funding This work was supported by the foundation ÅForsk (grant numbers 17–387; 19–323), Sweden's innovation agency VINNOVA (grant numbers 2017–02519; 2018–02383), the Swedish Foundation for Strategic Research (grant number FFL18-0173), the Swedish iron and steel producers' association Jernkontoret (grant number Prytziska fonden 2–2019), the Swedish Research Council for Environment, Agricultural Sciences, and Spatial Planning (Formas, 2017–00883), the Swedish Research Council (VR, 2017–03931 and 2019–03657), the Canada Research Chairs Program (grant number 950–233099), and the Wolfe-Western fellowship, Canada (grant number: 2020).

References

1. International Agency for Research on Cancer (2017) Welding, molybdenum trioxide and indium tin oxide (118). IARC, Lyon, France. Lancet Oncol 18(4):581–582
2. 't Mannetje A, Brennan P, Zaridze D, Szeszenia-Dabrowska N, Rudnai P, Lissowska J, Fabiánová E, Cassidy A, Mates D, Bencko V, Foretova L, Janout V, Fevotte J, Fletcher T, Boffetta P (2012) Welding and lung cancer in Central and Eastern Europe and the United Kingdom. Am J Epidemiol 175:706–14. https://doi.org/10.1093/aje/kwr358
3. Sørensen AR, Thulstrup AM, Hansen J, Ramlau-Hansen CH, Meersohn A, Skytthe A, Bonde JP (2007) Risk of lung cancer according to mild steel and stainless steel welding. Scand J Work Environ Health 33:379–386. https://doi.org/10.5271/sjweh.1157
4. Siew SS, Kauppinen T, Kyyronen P, Heikkila P, Pukkala E (2008) Exposure to iron and welding fumes and the risk of lung cancer. Scand J Work Environ Health 34:444–450. https://doi.org/10.5271/sjweh.1296
5. Kim JY, Chen JC, Boyce PD, Christiani DC (2005) Exposure to welding fumes is associated with acute systemic inflammatory responses. Occup Environ Med 62:157–163. https://doi.org/10.1136/oem.2004.014795
6. Riccelli MG, Goldoni M, Poli D, Mozzoni P, Cavallo D, Corradi M (2020) Welding fumes, a risk factor for lung diseases (Review). Int J Environ Res Public Health 17:2552. 32pp. https://doi.org/10.3390/ijerph17072552
7. Pesch B, Kendzia B, Hauptmann K, Van Gelder R, Stamm R, Hahn J-U, Zschiesche W, Behrens T, Weiss T, Siemiatycki J, Lavoué J, Jöckel K-H, Brüning T (2015) Airborne exposure to inhalable hexavalent chromium in welders and other occupations: estimates from the German MEGA database. Int J Hyg Envir Heal 218:500–506. https://doi.org/10.1016/j.ijheh.2015.04.004
8. Sjögren B (1980) A retrospective cohort study of mortality among stainless steel welders. Scand J Work Environ Health 6(3):197–200. https://doi.org/10.5271/sjweh.2616
9. Antonini JM, Taylor MD, Zimmer AT, Roberts JR (2004) Pulmonary responses to welding fumes: role of metal constituents. J Toxicol Env Heal A 67:233–249. https://doi.org/10.1080/15287390490266909
10. Antonini JM, Roberts JR, Stone S, Chen BT, Schwegler-Berry D, Chapman R, Zeidler-Erdely PC, Andrews RN, Frazer DG (2011) Persistence of deposited metals in the lungs after stainless steel and mild steel welding fume inhalation in rats. Arch Toxicol 85(5):487–498. https://doi.org/10.1007/s00204-010-0601-1

11. Occupational Safety & Health Administration (2017) National emphasis program – hexavalent chromium. OSHA, U.S. Department of labor, Washington DC. CPL 02–02–076
12. Zeidler-Erdely PC, Erdely A, Antonini JM (2012) Immunotoxicology of arc welding fume: worker and experimental animal studies. J Immunotoxicol 9(4):411–425. https://doi.org/10.3109/1547691X.2011.652783
13. Leonard SS, Chen BT, Stone SG, Schwegler-Berry D, Kenyon AJ, Frazer D, Antonini JM (2010) Comparison of stainless and mild steel welding fumes in generation of reactive oxygen species. Part Fibre Toxicol 7(1):32. https://doi.org/10.1186/1743-8977-7-32
14. Warming M, Lassen C, Christensen F, Kalberlah F, Oltmans J, Postle M, Vencovsky D (2018) Chromium (VI) in fumes from welding, plasma cutting and similar processes. Publications office of the European Union, Luxembourg 137pp. https://doi.org/10.2767/042168
15. Antonini JM (2003) Health effects of welding. Crit Rev Toxicol 33(1):61–103. https://doi.org/10.1080/713611032
16. Kimura S, Kobayashi M, Godai T, Minato S (1979) Investigations on chromium in stainless steel welding fumes. Weld J Res Suppl 58(7):195s–204s
17. Yoon CS, Paik NW, Kim JH (2003) Fume generation and content of total chromium and hexavalent chromium in flux-cored arc welding. Ann Occup Hyg 47(8):671–680. https://doi.org/10.1093/annhyg/meg063
18. Ferree S, Lake F (2012) Factors that affect hexavalent chromium emissions. Weld J 91(8):29–36
19. Hedberg YS, Wei Z, McCarrick S, Romanovski V, Theodore J, Westin EM, Wagner R, Persson K-A, Karlsson HL, Odnevall Wallinder I (2021) Welding fume nanoparticles from solid and flux-cored wires: solubility, toxicity, and role of fluorides. J Hazard Mater 413(7):125273. https://doi.org/10.1016/j.jhazmat.2021.125273
20. Palmer WG (1983) Effects of welding on health IV – effects of welding on human health. International Standard Book Number 0–87171–230-X. American Welding Society, Miami, FL. pp. 60
21. International Agency for Research on Cancer (2012) Nickel and nickel compounds (100C). IARC Monographs on the Evaluation of Carcinogenic Risks to Humans, Lyon, France. 100C:159–211. ISBN: 978–92–832–0135–9
22. Kawanishi S, Inue S, Oikawa S, Inoue S, Nishino K (2002) Distinct mechanisms of oxidative DNA damage induced by carcinogenic nickel subsulfide and nickel oxides. Environ Health Perspect 110(Suppl 5):789–791. https://doi.org/10.1289/ehp.02110s5789
23. Occupational Safety & Health Administration (2017) Nickel Standard No. 1910.1000. OSHA, Washington
24. ISO 15011-1 (2009) Health and safety in welding and allied processes – laboratory method for sampling fume and gases part 1: determination of fume emission rate during arc welding and collection of fume for analysis. European Committee for Standardization, Brussels, 28pp.
25. ISO 10882-1 (2012) Health and safety in welding and allied processes – sampling of airborne particles and gases in the operator's breathing zone part 1: sampling of airborne particles. European Committee for Standardization, Brussels, 50pp
26. AWS F1.2 (2013) Laboratory method for measuring fume generation rates and total fume emission of welding and allied processes. American Welding Society, Miami, FL. pp 26. ISBN: 978–0–87171–836–5
27. Mei X (2016) Characterization of stainless welding fume particles – influence of stainless steel grade, welding parameters and particle size. Degree project Materials Science and Engineering, KTH Royal Institute of Technology, Stockholm, Sweden. pp 66. http://kth.diva-portal.org/smash/get/diva2:944365/FULLTEXT01
28. Jenkins NT, Eagar TW (2005) Chemical analysis of welding fume particles. Weld J Res Suppl 84(6):87s–93s
29. Gonser MJ, Lippold JC, Dickinson DW, Sowards JW, Ramirez AJ (2010) Characterization of welding fume generated by high-Mn consumables. Weld J Res Suppl 89(2):25s–33s
30. Jenkins NT, Pierce WM-G, Eagar TW (2005) Particle size distribution of gas metal and flux cored arc welding fumes. Weld J Res Suppl 84(10):156s–163s
31. Berlinger B, Benker N, Weinbruch S, L'Vov B, Ebert M, Koch W, Ellingsen DG, Thomassen Y (2011) Physicochemical characterisation of different welding aerosols. Anal Bioanal Chem 399(11):1773–1780. https://doi.org/10.1007/s00216-010-4185-7
32. Falcone LM, Erdely A, Kodali V, Salmen R, Battelli LA, Dodd T, McKinney W, Stone S, Donlin M, Leonard HD, Cumpston JL, Cumpston JB, Andrews RN, Kashon ML, Antonini JM, Zeidler-Erdely PC (2018) Inhalation of iron-abundant gas metal arc welding-mild steel fume promotes lung tumors in mice. Toxicol 409(11):24–32. https://doi.org/10.1016/j.tox.2018.07.007
33. Cena LG, Keane MJ, Chisholm WP, Stone S, Harper M, Chen BT (2014) A novel method for assessing respiratory deposition of welding fume nanoparticles. J Occup Environ Hyg 11(12):771–780. https://doi.org/10.1080/15459624.2014.919393
34. Keane M, Siert A, Stone S, Chen B, Slaven J, Cumpston A, Antonini J (2012) Selecting processes to minimize hexavalent chromium from stainless steel welding. Weld J Res Suppl 91(9):247s–246s
35. Midander K, Pan J, Wallinder Odnevall I, Leygraf C (2007) Metal release from stainless steel particles in vitro-influence of particle size. J Environ Monit 9(1):74–81. https://doi.org/10.1039/b613919a
36. Sowards JW, Ramirez AJ, Lippold JC, Dickinson DW (2008) Characterization procedure for the analysis of arc welding fume. Weld J Res Suppl 87(3):76s–83s
37. ISO 12502-3 (2004) Workplace air – determination of metals and metalloids in airborne particulate matter by inductively coupled plasma atomic emission spectrometry – part 3: analysis. European Committee for Standardization, Brussels, 44pp.
38. Sowards JW, Ramirez AJ, Dickinson DW, Lippold JC (2010) Characterization of welding fume from SMAW electrodes – part II. Weld J Res Suppl 89(4):82s–90s
39. Heung W, Yun M-J, Chang DPY, Green PG, Halm C (2007) Emissions of chromium (VI) from arc welding. J Air Waste Manag Assoc 57(2):252–260. https://doi.org/10.1080/10473289.2007.10465314
40. Antonini JM, Lawryk NJ, Krishna Murthy GG, Brain JD (1999) Effect of welding fume solubility on lung macrophage viability and function in vitro. J Toxicol Environ Health Part A 58(6):343–363. https://doi.org/10.1080/009841099157205
41. McNeilly JD, Heal MR, Beverland IJ, Howe A, Gibson MD, Hibbs LR, MacNee W, Donaldson K (2004) Soluble transition metals cause the pro-inflammatory effects of welding fumes in vitro. Toxicol Appl Pharmacol 196(1):95–107. https://doi.org/10.1016/j.taap.2003.11.021
42. Minni E, Gustafsson TE, Koponen M, Kalliomäki P-L (1984) A study of the chemical structure of particles in the welding fumes of mild and stainless steel. J Aerosol Sci 15:57–68
43. Floros N (2018) Welding fume main compounds and structure. Weld World 62(1/2):311–316. https://doi.org/10.1007/s40194-018-0552-3
44. Sowards JW (2006) Method for sampling and characterizing arc welding fume particles. Weld World 50(9/10):40–54. https://doi.org/10.1007/BF03263444
45. Kobayashi M, Maki S, Hashimoto Y, Suga T (1978) Some considerations about the formation mechanism of welding fumes. Weld World 16(11/12):238–248
46. Levchenko OG (1998) Methods of reducing the generation of welding fumes (Review). Weld Int 12(9):747–752. https://doi.org/10.1080/09507119809452048

47. Dennis JH, French MH, Hewitt PJ, Mortazavi SB, Redding CAJ (2002) Control of occupational exposure to hexavalent chromium and ozone in tubular wire arc-welding processes by replacement of potassium by lithium or by addition of zinc. Ann Occup Hyg 46(1):33–42. https://doi.org/10.1093/annhyg/mef024
48. Dennis D, French M, Hewitt P, Mortazavi S, Redding A (1996) Reduction of hexavalent chromium concentration in fumes from metal cored arc welding by addition of reactive metals. Ann Occup Hyg 40(3):339–344. https://doi.org/10.1093/annhyg/mef024
49. Rajeswari VB, Paramashivan SS, Mohan S, Albert SK, Rahul M (2020) Effect of substituting fine rutile of the flux with nano TiO_2 on the improvement of mass transfer efficiency and the reduction of welding fumes in the stainless SMAW electrode. High Temp Mater Proc 39:117–123. https://doi.org/10.1515/htmp-2020-0030
50. Vishnu BR, Sivapirakasam SP, Satpathu KK, Shaju KA, Gopa C (2018) Influence of nano-sized flux materials in the reduction of the Cr(VI) in the stainless steel welding fumes. J Manuf Proc 34(8):713–720. https://doi.org/10.1016/j.jmapro.2018.07.009
51. Stern RM, Berlin A, Fletcher A, Hemminki K, Jarvisalo J, Peto J (1986) Summary report, International Conference on health hazards and biological effects of welding fumes and gases. Int Arch Occup Environ Health 57:237–246. https://doi.org/10.1007/BF00405791
52. Heile FR, Hill DC (1975) Particulate fume generation in arc welding processes. Weld J Res Suppl 54(7):201s–210s
53. Fiore SR (2006) Reducing exposure to hexavalent chromium in welding fumes. Weld J 85(8):38–42
54. Mei N, Belleville L, Cha Y, Olofsson U, Odnevall Wallinder I, Persson K-A, Hedberg YS (2018) Size-separated particle fractions of stainless steel welding fume particles – a multi-analytical characterization focusing on surface oxide speciation and release of hexavalent chromium. J Hazard Mater 342:527–535. https://doi.org/10.1016/j.jhazmat.2017.08.070
55. McCarrick S, Romanovski V, Wei Z, Westin EM, Persson K-A, Trydell K, Wagner R, Odnevall I, Hedberg YS, Karlsson HL (2021) Genotoxicity and inflammatory potential of stainless steel welding fume particles – an *in vitro* study on standard vs Cr(VI)-reduced flux-cored wires and the role of released metals. Arch Toxicol 95(7):2961–2975. https://doi.org/10.1007/s00204-021-03116-x
56. Järvelä M, Kauppi P, Tuomi T, Luukkonen R, Lindholm H, Nieminen R, Moilanen E, Hannu T (2013) Inflammatory response to acute exposure to welding fumes during the working day. Int J Occup Med Environ Health 26(2):220–229. https://doi.org/10.2478/s13382-013-0097-z
57. Badding MA, Fix NR, Antonini JM, Leonard SS (2014) A comparison of cytotoxicity and oxidative stress from welding fumes generated with a new nickel-, copper-based consumable versus mild and stainless steel-based welding in RAW 264.7 mouse macrophages. PLOS ONE 9(6):e101310. 11pp. https://doi.org/10.1371/journal.pone.0101310
58. Pascal LE, Tessier DM (2004) Cytotoxicity of chromium and manganese to lung epithelial cells in vitro. Toxicol Lett 147(2):143–151. https://doi.org/10.1016/j.toxlet.2003.11.004
59. Hetland RB, Myhre O, Låg M, Hongve D, Schwarze PE, Refsnes M (2001) Importance of soluble metals and reactive oxygen species for cytokine release induced by mineral particles. Toxicol 165(2–3):133–144. https://doi.org/10.1016/s0300-483x(01)00418-8
60. Shoeb M, Kodali V, Farris B, Bishop LM, Meighan T, Salmen R, Eye T, Roberts JR, Zeidler-Erdely P, Erdely A, Antonini JM (2017) Evaluation of the molecular mechanisms associated with cytotoxicity and inflammation after pulmonary exposure to different metal-rich welding particles. Nanotoxicol 11(6):725–736. https://doi.org/10.1080/17435390.2017.1349200
61. McCarrick S, Wei Z, Moelijker N, Derr R, Persson K-A, Hendriks G, Odnevall Wallinder I, Hedberg YS, Karlsson HL (2019) High variability in toxicity of welding fume nanoparticles from stainless steel in lung cells and reporter cell lines: the role of particle reactivity and solubility. Nanotoxicol 13(10):1293–1309. https://doi.org/10.1080/17435390.2019.1650972
62. Westin EM, McCarrick S, Laundry-Mottiar L, Wei Z, Wagner R, Persson K-A, Trydell K, Odnevall I, Karlsson HL, Hedberg YS (2021) New weldable 316L stainless flux-cored wires with reduced Cr(VI) fume emissions. Part 2 – Round robin creating fume emission data sheets. In press: Weld World. https://doi.org/10.1007/s40194-021-01189-x
63. ISO 15011–4 (2018) Health and safety in welding and allied processes – laboratory method for sampling fume and gases – part 4: fume data sheets. European Committee for Standardization, Brussels, Belgium. 24pp
64. Biesinger MC, Payne BP, Grosvenor AP, Lau LWM, Gerson AR, Smart RSC (2011) Resolving surface chemical states in XPS analysis of first row transition metals, oxides and hydroxides: Cr, Mn, Fe, Co and Ni. Appl Surf Sci 257(7):2717–2730. https://doi.org/10.1016/j.apsusc.2010.10.051
65. Di Bucchianico S, Cappellini F, Le Bihanic F, Zhang Y, Dreij K, Karlsson HL (2017) Genotoxicity of TiO_2 nanoparticles assessed by mini-gel comet assay and micronucleus scoring with flow cytometry. Mutagenesis 32(1):127–137. https://doi.org/10.1093/mutage/gew030
66. Cohen MD, Kargacin B, Klein CB, Costa M (1993) Mechanisms of chromium carcinogenicity and toxicity. Crit Rev Toxicol 23(3):255–281. https://doi.org/10.3109/10408449309105012
67. Salnikow K, Zhitkovich A (2008) Genetic and epigenetic mechanisms in metal carcinogenesis and cocarcinogenesis: nickel, arsenic, and chromium. Chem Res Toxicol 21(1):28–44. https://doi.org/10.1021/tx700198a
68. Westin EM, Schnitzer R, Ciccomascolo F, Maderthoner A, Grönlund K, Runnsjö G (2016) Austenitic stainless steel bismuth-free flux-cored wires for high-temperature applications. Weld World 60(6):1147–1158. https://doi.org/10.1007/s40194-016-0376-y
69. Höfer K, Kusch M, Mayr P (2015) Minimierung der Emissionsraten beim MSG-Schweißen mit Fülldrahtelektroden. Final report Aif-Vorhaben Nr. 17.557B. Technical University Chemnitz. pp. 62
70. Kirichenko KY, Agoshkov AI, Drozd VA, Gridasov AV, Kholodov AS, Kobylyakov SP, D. Yu. Kosyanov DY, Zakharenko AM, Karabtsov AA, Shimanskii SR, Stratidakis AK, Mezhuev YO, Tsatsakis AM, Golokhvast KS (2018) Characterization of fume particles generated during arc welding with various covered electrodes. Scientific Reports 8(1):17169 9pp. https://doi.org/10.1038/s41598-018-35494-1
71. Yu IJ, Song KS, Maeng SH, Kim SJ, Sung JH, Han JH, Chung YH, Cho MH, Chung KH, Han KT, Hyun JS, Kim KJ (2004) Inflammatory and genotoxic responses during 30-day welding-fume exposure. Toxicol Lett 154(1–2):105–115. https://doi.org/10.1016/j.toxlet.2004.07.009
72. Antonini JM, Leonard SS, Roberts JR, Solano-Lopez C, Young S-H, Shi X, Taylor MD (2005) Effect of stainless steel manual metal arc welding fume on free radical production, DNA damage, and apoptosis induction. Mol Cell Biochemi 279:17–23. https://doi.org/10.1007/s11010-005-8211-6
73. Wild P, Bourgkard E, Paris C (2009) Lung cancer and exposure to metals: the epidemiological evidence. Methods Mol Biol 472:139–167. https://doi.org/10.1007/978-1-60327-492-0_6
74. Karlsson HL, Cronholm P, Gustafsson J, Möller L (2008) Copper oxide nanoparticles are highly toxic: a comparison between metal oxide nanoparticles and carbon nanotubes. Chem Res Toxicol 21(9):1726–1732. https://doi.org/10.1021/tx800064j

75. Kalliomäki PL, Junttila ML, Kalliomäki K, Lakomaa EL, Kivelä R (1983) Comparison of the retention and clearance of different welding fumes in rat lungs. Am Ind Hyg Assoc J 44(10):733–738. https://doi.org/10.1080/15298668391405652
76. Falcone LM, Erdely A, Salmen R, Keane M, Battelli L, Kodali V, Bowers L, Stefaniak AB, Kashon ML, Antonini JM, Zeidler-Erdely PC (2018) Pulmonary toxicity and lung tumorigenic potential of surrogate metal oxides in gas metal arc welding-stainless steel fume: iron as a primary mediator versus chromium and nickel. PLOS ONE 13(12):e0209413. https://doi.org/10.1371/journal.pone.0209413
77. Ali SF, Duhart HM, Newport GD, Lipe GW, Slikker W (1995) Manganese-induced reactive oxygen species: comparison between Mn^{+2} and Mn^{+3}. Neurodegeneration 4(3):329–334. https://doi.org/10.1016/1055-8330(95)90023-3
78. Keane M, Stone S, Chen B (2010) Welding fume from stainless steel gas metal arc processes contain multiple manganese chemical species. J Environ Monit 12(5):1133–11404. https://doi.org/10.1039/B922840C
79. Antonini JM, Keane M, Chen BT, Stone S, Roberts JR, Schwegler-Berry D, Andrews RN, Frazer DG, Sriram K (2011) Alterations in welding process voltage affect the generation of ultrafine particles, fume composition, and pulmonary toxicity. Nanotoxicol 5(4):700–710. https://doi.org/10.3109/17435390.2010.550695
80. Sowards JW, Lippold LC, Dickinson DW, Ramirex AJ (2008) Characterization of weld fume from SMAW electrodes – part I. Weld J Res Suppl 87(4):106s–112s
81. Jönsson LS, Tinnerberg H, Jacobsson H, Andersson U, Axmon A, Nielsen J (2015) The ordinary work environment increases symptoms from eyes and airways in mild steel welders. Int Arch Occup Environ Health 88:1131–1140. https://doi.org/10.1007/s00420-015-1041-2
82. Sjögren B, Fossum T, Lindh T, Weiner J (2002) Welding and ischemic heart disease. Int J Occup Environ Health 8(4):309–311. https://doi.org/10.1179/oeh.2002.8.4.309
83. Zimmer AT, Baron PA, Biwas P (2002) The influence of operating parameters on number-weighted aerosol size distribution generated from a gas metal arc welding process. J Aerosol Sci 33:519–531. https://doi.org/10.1039/B202337G
84. Lindahl M, Leanderson P, Tagesson C (1998) Novel aspect on metal fume fever: zinc stimulates oxygen radical formation in human neutrophils. Hum Exp Toxicol 17(2):105–110. https://doi.org/10.1177/096032719801700205
85. Hartwig A, Heederik D, Kromhout H, Levy L, Papameletiou D, Klein CL (2017). Recommendation from the scientific committee for occupational exposure limits. Chromium VI compounds. SCOEL/REC/386 European Commission, Employment, Social Affairs and Inclusion. 58pp. https://op.europa.eu/en/publication-detail/-/publication/75d27056-893f-11e7-b5c6-01aa75ed71a1/language-en. Accessed 20 June 2021.
86. American Conference of Governmental Industrial Hygienists (2001) Documentation of the threshold limit values for chemical substances, 7th edn. ACGIH, Cincinnati
87. National Institute for Occupational Safety and Health (2013) Criteria for a recommended standard: occupational exposure to hexavalent chromium. DHSS, NIOSH, Washington
88. Occupational Safety & Health Administration (2006) Chromium (VI). OSHA, Washington
89. Gomes JFG, Albuquerque PCS, Miranda RMM, Vieira MTF (2012) Determination of airborne nanoparticles from welding operations. J Toxicol Environ Health Part A 75(13–15):747–755. https://doi.org/10.1080/15287394.2012.688489
90. Liu HH, Wu YC, Chen HL (2007) Production of ozone and reactive oxygen species after welding. Arch Environ Contam Toxicol 53(4):513–518. https://doi.org/10.1007/s00244-007-0030-1
91. Wagner R, Sievert E, Schein J, Hussary N, Jäckel S (2018) Shielding gas influence on emissions in arc welding. Weld World 62(3):647–652. https://doi.org/10.1007/s40194-018-0573-y
92. Wagner R, Siewert E, Schein J, Hussary N, Eichler S, Fehrenbach L, Pfreuntner M (2021) Einfluss von Schutzgas auf die Emissionen beim Lichtbogenschweißen. Paper to be presented in September at the Proc DVS Congress Expo Große Schweißtechnische Tagung 2021, Essen, Germany
93. Höfer K, Kusch M, Mayr P (2015) Flux cored arc welding – determination and reduction of fume emission rates. Paper presented at the 68th IIW Annual Assembly, Helsinki, Finland. IIW Doc. VIII-2199–15. pp. 7
94. Yamamoto E, Yamazaki K, Suzuki K, Koshiishi G (2010) Effect of fume ratio in flux-cored wire on wire melting behavior and fume emission rate. Weld World 54(5/6):154–159. https://doi.org/10.1007/BF03263501
95. Böhler Welding (2021) Stainless steel and nickel-base cored wires to join stainless steel. 40pp. https://www.voestalpine.com/welding/Services/Downloads